Geophys. Astrophys. Fluid Dynamics, Vol. 89, pp. 1–22
Reprints available directly from the publisher
Photocopying permitted by license only

EXPERIMENTS ON BUOYANT PLUMES IN A ROTATING CHANNEL

JOHN W. M. BUSH[a,*] and ANDREW W. WOODS[b]

[a] *Institute of Theoretical Geophysics, Department of Applied Mathematics and Theoretical Physics, University of Cambridge, Cambridge CB3 9EW, U.K.;*
[b] *Centre for Environmental and Geophysical Flows, School of Mathematics, University of Bristol, BS8 1TW, U.K.*

(Received 6 November 1997; In final form 9 March 1998)

The influence of bounding geometry and rotation on the discharge of buoyant fluid from a turbulent axisymmetric plume in an open-ended channel is examined through an experimental study. Both homogenous and stratified ambients are considered. In the non-rotating channel, the plume rises and spreads as a pair of counterflowing gravity currents at either the free surface (in a homogenous ambient) or at the plume's level of neutral buoyancy (in a stratified fluid). Scaling laws and accompanying experiments indicate that in a homogeneous environment, the surface gravity currents emerging from a channel of width W and depth H have a depth h which is independent of plume source conditions:

$$h = (0.13 \pm 0.02) H^{5/3} W^{-2/3}.$$

When the ambient is stratified and characterised by a constant Brunt-Vaisala frequency N, the current intruding at its neutral height Z_n has a uniform thickness

$$h = (1.1 \pm 0.2) B^{3/8} N^{-9/8} W^{-1/2},$$

where B is the plume buoyancy flux. These results were found to be robust for high Reynolds number gravity currents, but broke down for $Re < 100$ when viscous effects became important. Moreover, when the channel was sufficiently narrow, $W < (H/3, Z_N/3)$ the results broke down in a manner consistent with the channel walls acting to suppress entrainment into the plume.

When the system is rotating, the mode of discharge is characterized in terms of the relative magnitudes of the channel width and the maximum radius attainable by the anticyclonic plume vortex before the onset of instability. In the homogeneous environment, the plume vortex takes a columnar form, which may attain a radius,

*Address for Correspondence: Department of Mathematics, Massachusetts Institute of Technology, Cambridge MA 02139, U.S.A. e-mail: Bush@math.mit.edu

$R_{max} = 8L_f$, where $L_f = B^{1/4}/f^{3/4}$ is the rotational lengthscale and f is twice the rotation rate of the system. In the stratified environment, with $N \gg f$, the plume vortex takes a lenticular form which may attain a radius of $R_{max} = NZ_n/f$ before going unstable. For $W \gg R_{max}$, the flow is unsteady, characterised by the pulsatile shedding of discrete vortices from the central plume. For $W \ll R_{max}$, the flow is steady, characterised by a pair of counterflowing geostrophic gravity currents.

Particular attention is given to the steady geostrophic regime in the homogeneous environment, from which it is possible to infer the volume flux of the fluid exiting the channel from the shape of the boundary currents, and so to infer the influence of rotation on the rate of entrainment into a turbulent plume. The experiments indicate that the volume flux exiting in the form of gravity currents, Q_g, is related to that which would emerge at the free surface in the absence of rotation, Q_0, through

$$\frac{Q_g}{Q_0} = (5.0 \pm 1.0) \left(\frac{L_f}{H} \right)^{5/3}.$$

This scaling result is consistent with the simple physical model of the plume entraining as it would in the absence of rotation up to a distance $2.6L_f$ above the source, above which rotation serves to entirely suppress entrainment into the plume.

Keywords: Turbulent plume; channel; rotation; stratification

1. INTRODUCTION

The influence of the Earth's rotation on the dynamics of turbulent plumes is a problem of interest in a wide variety of geophysical problems, including deep-ocean mixing induced by either surface cooling in the open ocean or freezing events in the polar seas, hydrothermal plumes at the seafloor, and violent mixing events in the Earth's atmosphere. The interaction of buoyant plumes, rotation and bounding geometry is also a problem with a number of oceanographic applications, including meltwater run-off from the base of glaciers into fjords, hydrothermal plumes in axial valleys, and deep-ocean mixing near continental margins. We here consider the combined influence of rotation and a bounding channel geometry on the dynamics of turbulent plumes in both homogeneous and stratified environments. In addition to providing insight into the aforementioned oceanic problems, the chosen channel geometry allows us to make a fundamental deduction concerning the influence of rotation on entrainment into turbulent plumes.

The influence of background rotation (with angular speed $f/2$) and ambient stratification (characterized by a Brunt-Vaisala frequency N)

on the dynamics of buoyant plumes has received considerable recent attention (Helfrich and Battisti, 1991; Lavelle, 1997; Speer and Marshall, 1995). In typical oceanic applications, particularly those involving hydrothermal plumes, $N/f \gg 1$; consequently, the plume fluid rises to its level of neutral buoyancy before being influenced by the Earth's rotation. There also exist well-mixed regions of the oceans where N is considerably smaller, so that the dynamics is more strongly influenced by rotation. As a result of the dynamic influence of the Coriolis force, the radial motions associated with both the spreading of the neutral cloud and entrainment into the plume are suppressed. The neutral cloud assumes the form of a lenticular anticyclonic vortex, and the underlying plume is cyclonic. The neutral cloud is in geostrophic balance, with the radial pressure force being balanced by the opposing Coriolis force associated with the anticyclonic swirling motion; consequently, the height to width ratio, h/R, of the neutral cloud is related to f/N by an order one constant (Helfrich and Battisti, 1991). The suppression of radial entrainment results in fluid from the neutral cloud being re-entrained into the lower part of the plume; consequently, the fluid entrained into the plume is less dense than it would be in the absence of rotation, and the neutral cloud encroaches vertically (Speer and Marshall, 1995). The plume system in a rotating stratified ambient thus contains a circulating cell reminiscent of 'filling box' flows (Baines and Turner, 1969); however, in the rotating case, the bounding 'box' is a cylinder with a radius prescribed by the system rotation.

The neutral cloud grows to a critical radius

$$R_r = NZ_n/f = 2.5B^{1/4}N^{1/4}f^{-1} \tag{1}$$

after a time on the order of 100 N/f rotation periods before going unstable in a manner which depends on the magnitude of N/f. For $N/f > 2$, the neutral cloud simply drifts off the source as a single anticyclonic monopolar vortex, while for $N/f < 2$, the neutral cloud sheds dipolar vortices which propagate away from the source (Helfrich and Battisti, 1991). When $N/f \gg 1$, the continuous discharge of buoyant plume fluid results in the formation of a series of flat lenticular anticyclonic monopolar vortices which drift away from the source in turn.

The rate of entrainment into a turbulent plume is traditionally determined by examining the flow associated with an isolated plume discharging into a confined region (Baines and Turner, 1969). The plume fluid entrains and mixes with the ambient as it rises and spreads out at the free surface, giving rise to a horizontal interface between plume and ambient fluids. As time passes, a stratification develops within the upper layer, and the interface descends. The rate of descent of the interface in this 'filling box' system may be used to calculate the entrainment coefficient, α, defined by the ratio of the mean vertical velocity within the plume to the mean radial inflow velocity. Baines and Turner (1969) determined $\alpha = 0.1$. Note that this technique is not readily adaptable to the rotating plume system, since the vertical motion of the interface will induce vigorous swirling motions which are cyclonic and anticyclonic, respectively, below and above the interface. Consequently, it is not straightforward to deduce the impact of system rotation on the rate of entrainment into a turbulent plume using the traditional filling box technique. We here introduce an alternative method which is possible only by virtue of the open-ended channel geometry chosen for our experiments.

In this study we combine the description of a plume in a rotating stratified ambient with a new experimental study in order to draw a simple physical picture of a plume discharging into a rotating stratified ambient bound in a channel. In Section 2, we describe the experimental technique employed in our study. The scaling and accompanying experimental results describing a plume discharging into a channel in a non-rotating homogeneous ambient are presented in Section 3. The influence of rotation on the flows is investigated in Section 4. In Section 5, we consider plume discharge into a stratified ambient bound in a channel. We conclude in Section 6 by discussing the implications of this study for models of hydrothermal discharge within axial valleys.

2. EXPERIMENTAL TECHNIQUE

The experimental apparatus used in this study is illustrated in Figure 1. An open-ended plexiglass channel of length $L = 60$ cm and variable width was submerged in a reservoir mounted on a rotating turntable.

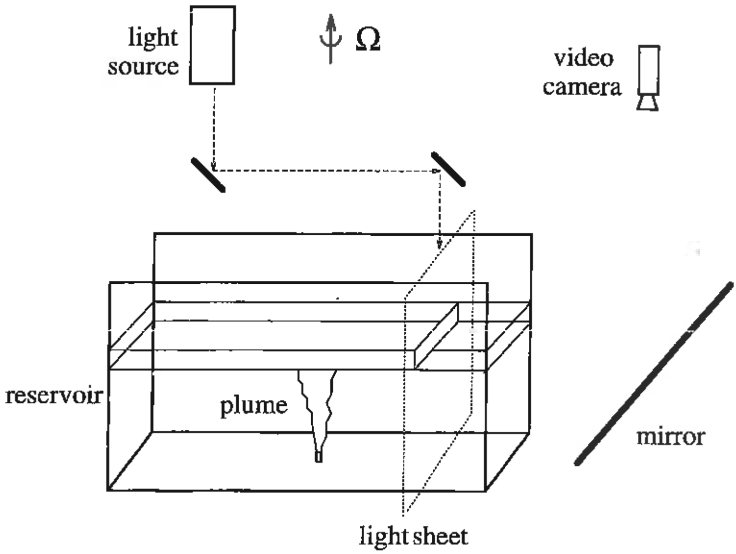

FIGURE 1 The experimental apparatus. The channel was contained within a cylindrical tank of diameter 1 m and depth 50 cm. Different cross sections of the channel could be examined by making use of a sliding mirror arrangement.

For the case of a homogeneous ambient, the reservoir was filled with saltwater before being spun-up, a process which was expedited by the presence of the channel walls, and which generally took approximately half an hour. For a uniformly statified ambient, the reservoir was filled while rotating using a double-bucket system which fed saltwater into the rotating frame through a sliding tube attached at the rotation axis and entered the tank through a floating sponge device. Dyed fresh water was released from a source reservoir on the top of the turntable, and the flow rate monitored by a flowmeter. The source fluid was released from a point source fixed in the center of the channel base and rises as a turbulent plume until it reaches the free surface, where the plume fluid spreads in either direction along the channel as a pair of gravity currents. The plume sources were specifically designed to promote turbulence in the plume even at low flow rates, and so to minimize jet lengths (Linden and Cooper, 1996). The volume flux rates were typically 1 cc/s, and the associated jet lengths were no greater than 1 cm in any of the experiments reported. Profiles of the plume and gravity currents were obtained by using fluorescein dye and illuminating the desired cross-sectional plane with a light sheet. The position of the light sheet could be varied during the course of an experiment with a sliding mirror apparatus. The flows were visualized by way of traditional particle and dye tracking techniques.

3. NON-ROTATING AMBIENT

We first consider the case of a plume discharging into a homogeneous ambient of depth H bound within a non-rotating channel of width W and apply simple scaling arguments appropriate for turbulent plumes (Morton *et al.*, 1956) in order to deduce the depth of the gravity current exiting the channel. For the case of a homogeneous ambient, the plume rises to the free surface $z = H$, where the properties of the plume fluid are expressed in terms of the source buoyancy flux B through:

$$Q_p(H) \sim B^{1/3} H^{5/3}, \quad g'(H) \sim B^{2/3} H^{-5/3}. \tag{2}$$

The gravity currents exiting the channel may be characterized by their Reynolds numbers,

$$Re = \frac{Uh}{\nu} = \frac{Q}{W\nu}, \tag{3}$$

where $Q = UhW$ is the volume flux in each gravity current and ν denotes the fluid viscosity. Note that Re does not depend on distance r from the source for a two-dimensional current.

In our experiments, the gravity currents exiting either end of the channel were characterized by $Re \sim 500-1000$, and their exit velocities could be expressed in terms of the their depth h through $U \sim (g'h)^{1/2}$. Conservation of volume requires that $Q_p(H) = 2UWh$, from which it may be inferred from (2) that

$$\frac{h}{H} = C_1 \left(\frac{H}{W}\right)^{2/3}. \tag{4}$$

The gravity current depth h is predicted to be independent of the plume buoyancy flux B, and to depend exclusively on the depth H and width W of the channel. The validity of this simple scaling was examined with a series of experiments.

The depth of the gravity currents was measured by illuminating the flow in a plane parallel to the bounding walls, which made it possible to observe variations in gravity current depth with distance from the source. The gravity current depth was found to be constant for distances greater than H from the source. For $x < H$, the flow was irregular, and the gravity currents were relatively shallow. This region corresponds to the 'zone of rings' identified by Linden and Simpson (1994) in their study of turbulent plumes impinging on a free surface. The depth also decreased near the end of the channel; however, for $H < x < (L-W)$, the gravity currents had constant depth, and it is in this region that measurements were made.

The results of our experimental study are presented in Figure 2. Six channel widths were used, and the effective depth of the channel

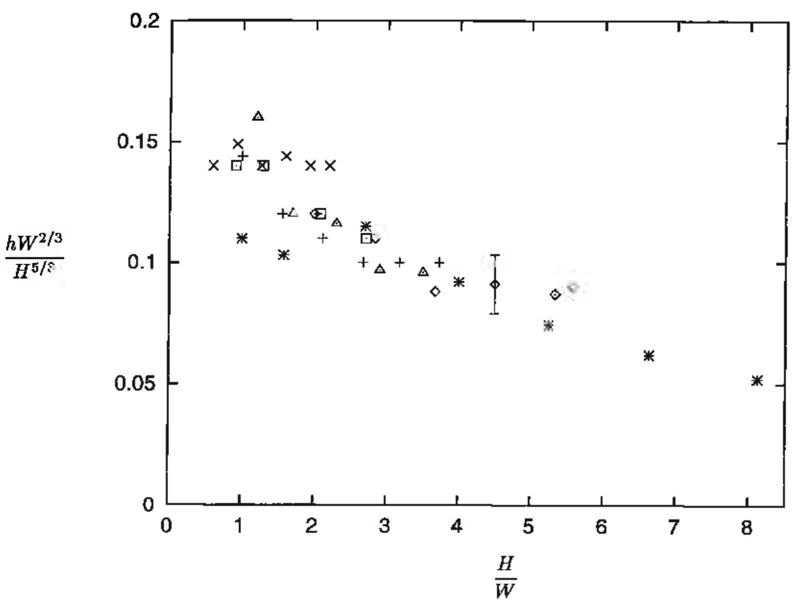

FIGURE 2 The dependence of the depth of the gravity current, formed by a turbulent buoyant plume discharging into a homogeneous fluid bound by an open-ended nonrotating channel, on the channel geometry. Symbols $*$, $\diamond$, $+$, Δ, $\square$, $\times$ correspond to channels of width 4, 6, 9, 10, 12 and 15 cm, respectively. A characteristic error bar is shown.

altered by changing the water level. For short channels $H/W<2$, the experiments confirm the scaling (4) and indicate that $C_1=0.13\pm0.02$. This limiting short channel result is consistent with the observations made by Linden and Simpson (1994), who measured the buoyancy flux emerging from a plume intruding on an interface to be $Q_0=B^{1/3}H^{5/3}/8$, from which it may be inferred that $C_1=0.125$. For narrow channels $H/W>3$, the scaling does not appear to be as robust, and the constant of proportionality is observed to decrease monotonically with increasing H/W. This trend is consistent with diminished entrainment into the plume associated with the influence of the channel walls.

4. ROTATING AMBIENT

We proceed by considering the influence of rotation on a buoyant plume discharging into a homogeneous unbounded system. Non-rotating plume scaling indicates the dependence on B and distance z above the source of the mean vertical plume speed $w \sim B^{1/3}z^{-1/3}$ and plume width $b \sim z$ (Morton *et al.*, 1956). The Taylor–Proudman Theorem requires that in a homogeneous fluid in which flow is geostrophic, there may be no gradients in velocity in the direction parallel to the rotation axis. Consequently, we anticipate that the strongly z-dependent flow structure associated with a turbulent plume will be strongly influenced by rotation. The influence of rotation on the rising plume may be characterized by the plume Rossby number, $Ro=w/(bf) \sim B^{1/3}f^{-1}z^{-4/3}$, which necessarily decreases with height above the source. The rotational lengthscale $L_f=B^{1/4}/f^{3/4}$ (Fernando *et al.*, 1991; Maxworthy and Narimousa, 1994) corresponds to the height at which $Ro=1$: for $z>L_f$, the plume dynamics is dominated by rotation. Our experiments verify that the radial spread of a rising plume is suppressed at a distance comparable to L_f from the source, above which the plume assumes an anticyclonic columnar structure of characteristic radius L_f in which vertical speeds are negligibly small, in compliance with the Taylor–Proudman theorem. The columnar plume eventually goes unstable, shedding a pair of columnar vortices in a manner analogous to that arising in a rotating stratified fluid (Griffiths and Linden, 1981).

When the system is rotating, two additional lengthscales thus arise, namely, the rotational lengthscale, L_f and the Ekman boundary layer thickness $\delta = \sqrt{\nu/\Omega}$. In all experiments reported, the Ekman length was much smaller than the other lengthscales in the problem; consequently, we neglect the influence of flows associated with Ekman transport. We likewise neglect the influence of Stewartson layers, the viscous boundary layers which must arise on the side wall. The mode of discharge in the homogeneous rotating ambient may then be characterized in terms of the relative magnitudes of the three remaining lengthscales in the problem; specifically, W, H and L_f.

4.1. Mode of Discharge

The purpose of the experimental study was to characterize the qualitative effect of rotation rate and channel geometry on the mode of discharge of plume fluid from the channel. Three distinct modes of discharge were identified, and are illustrated qualitatively in Figure 3. In the absence of rotation, the plume fluid rose, impinged on the free surface and exited as uniform-depth gravity currents (Fig. 3a). When the system was rotating, the gravity current dynamics were influenced by rotation: the currents were driven up against one of the channel walls by the Coriolis force (Fig. 3b). The system rotation likewise had an influence on the plume, which was strongly cyclonic in its lower entraining regions, and anticyclonic in its upper spreading regions. If the system rotation was sufficiently large, the gravity currents assumed the form of counterflowing boundary currents confined to one side of the channel. At the largest rotation rates considered, the plume became unstable before the gravity currents were able to extend to the channel walls (Fig. 3c). The plumes in this regime were strongly columnar, and shed pairs of anticyclonic columnar structures which collided with the walls before slowly exiting the channel. The flow in this latter regime was thus unsteady and pulsatile in character.

The dependence of mode of discharge on system parameters is indicated in Figure 4. For tall narrow channels, $W/H < 0.2$, the plume hits one or both walls before reaching the free surface. At the lowest rotation rates, the gravity current does not have a chance to adjust to geostrophy before exiting the channel. As rotation rate increases, the current adjusts to a steady geostrophic form before exiting the

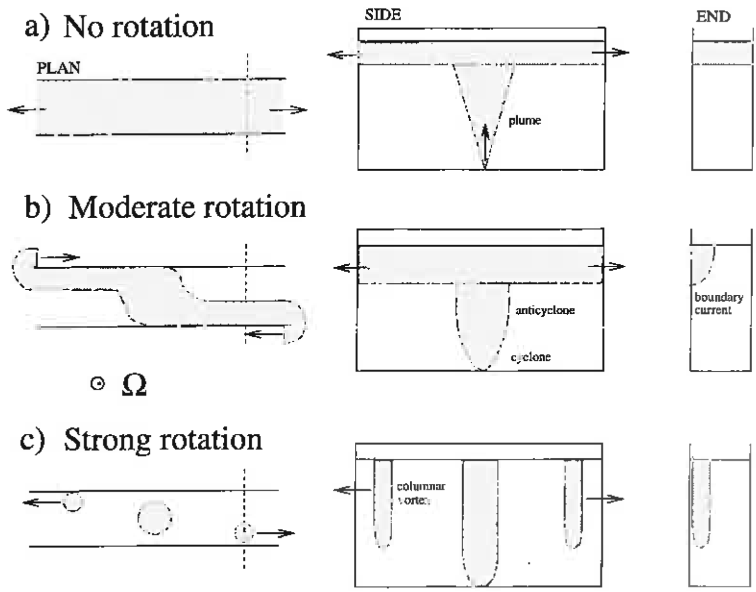

FIGURE 3 A schematic illustration of the three modes of discharge of plume fluid from a rotating channel environment. (a) In the absence of rotation, the plume fluid rises to the free surface and exits in the form of two counterflowing gravity currents of uniform depth. (b) In the moderate rotation regime, the plume consists of a cyclonic base (the entraining region) beneath an anticyclonic vortex (the spreading region). The plume fluid exits the channel in the form of geostrophically balanced boundary currents. (c) At the highest rotation rates, the plume vortex goes unstable, giving rise to a periodic release of columnar vortices which propagate out of the channel.

channel. In this case, the exiting plume fluid may take the form of either sloping currents spanning the entire channel, or a pair of counterflowing boundary currents confined to either wall. The most important feature of Figure 4 is the delineation between the steady geostrophic boundary current regimes and the unsteady pulsatile flows. We expect the pulsatile flows to arise when the rotational length L_f, which characterizes the maximum plume column radius, is less than the channel width. Indeed, Figure 4 indicates that pulsatile flow arises when

$$W > (8.0 \pm 1.0)L_f. \tag{5}$$

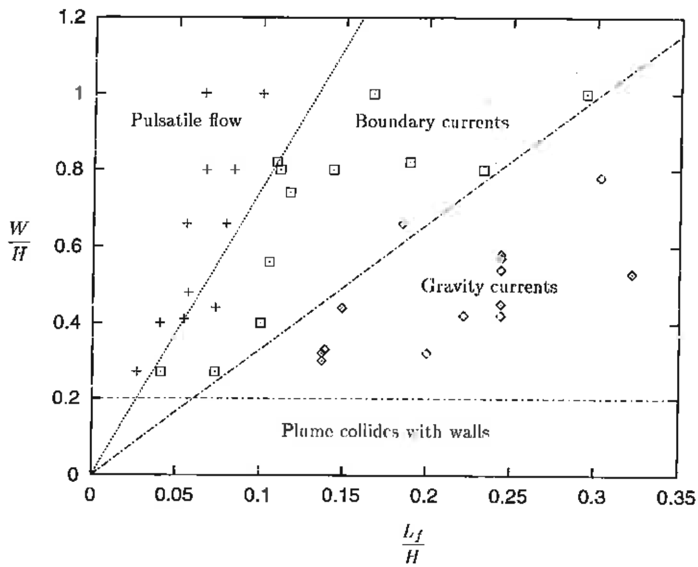

FIGURE 4 The dependence of mode of plume discharge on rotation rate. For $W/H < 0.2$, the plume hits one of the channel walls before reaching the surface. At weak rotation rates, $L_f > W/20$, denoted by ◇, the gravity current exiting the channel spans the entire channel width. At intermediate rotation rates, $W/20 < L_f < W/8$, denoted by □, the plume fluid exits the channel in the forms of steady geostrophic boundary currents. For $L_f < W/8$, denoted by +, the flow is characterised by the unsteady pulsatile release of columnar vortices.

For $L_f > W/8$, the plume column is stabilized by the channel walls, which allow plume fluid to exit the channel in geostrophic boundary currents and so prevent the column from growing to the point of instability.

4.2. Geostrophic Gravity Current

The most important mode of discharge for the purposes of our study arises when the plume fluid exits the channel in the form of steady geostrophic boundary currents (Griffiths and Hopfinger, 1983; Stern *et al.*, 1982). In this regime, it is possible to infer the volume flux exiting the channel from the cross-sectional shape of the boundary currents, and so to characterize the influence of rotation on entrainment into a turbulent plume.

We consider the dynamics of a quasi-steady gravity current of density $\rho - \Delta\rho$ translating along a wall $x=0$ at a free surface $z=0$ in a rapidly rotating fluid of uniform density ρ. We assume that the flow is unidirectional $\mathbf{v}=u(x)\hat{\mathbf{y}}$ and that the fluid motions are governed by a geostrophic balance

$$-\nabla p_d = f\hat{\mathbf{z}} \times \mathbf{v} \tag{6}$$

which in component form yields

$$\frac{\partial p_d}{\partial y} = 0, \quad \frac{\partial p_d}{\partial x} = -\rho f u(x). \tag{7}$$

The pressure is independent of the cross-channel variable x; consequently, the pressure distribution within the current may be obtained by continuity at the interface, which yields

$$p_d(x) = \rho g' h(x), \tag{8}$$

where $g' = g\Delta\rho/\rho$ is the reduced gravity of the gravity current and $h(x)$ defines the gravity current depth. Differentiating with respect to x and using (7) indicates that the velocity within the gravity current is proportional to the local slope of the interface:

$$u(y) = -\frac{g'}{f}\frac{dh}{dx}. \tag{9}$$

Consequently, the volume flux within the gravity current may be expressed as

$$Q_g = \int_0^W u(x)\, h(x) dx = \frac{g'}{2f}\,[h^2(0) - h^2(W)]. \tag{10}$$

Using the conservation of buoyancy makes it possible to eliminate g' and so to express Q_g in an alternate form

$$Q_g = \frac{B^{1/2}}{2f^{1/2}}\,[h^2(0) - h^2(W)]^{1/2}, \tag{11}$$

which depends exclusively on the source buoyancy and the cross-sectional profile of the gravity current.

The density of buoyant fluid emerging from an isolated jet or plume and impinging on a lower boundary a distance H from the source in an unbounded system has been considered by Linden and Simpson (1994). In the limit of a pure plume, they deduced that the reduced gravity of the fluid emerging as an axisymmetric gravity current is $g' = 4B^{2/3}H^{-5/3}$. This in turn implies that the associated volume flux $Q_0 = B^{1/3}H^{5/3}/8$. If the rotation had no impact on the plume, we would expect a total volume flux Q_0 to emerge from the gravity currents. In what follows, we demonstrate that such is not the case.

When the plume fluid exits the channel in the form of two counterflowing geostrophic gravity currents, it is possible to infer the volume flux exiting the channel from the cross-sectional gravity current profiles via (11), and so to quantify the influence of rotation on entrainment into the plume. Figure 5 illustrates the cross-sectional profile of a boundary current exiting the channel. It should be noted that the boundary currents were steady and laminar to a good approximation, and characterized by Reynolds numbers in the range 300 – 800. Figure 6 illustrates the dependence of the volume flux, Q_g, exiting the channel in the form of the steady boundary currents, on rotation rate. The rotation clearly has a strong impact on the entrainment into the plume: at the highest rotation rate, the volume flux emerging from the channel is reduced by more than a factor of

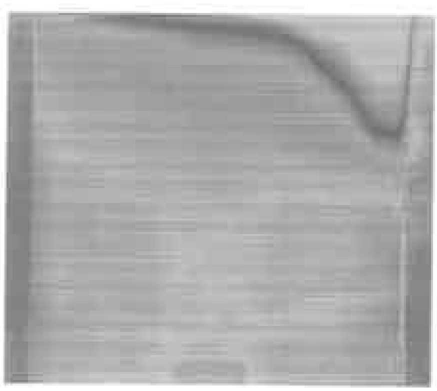

FIGURE 5 Cross-sectional profile of a boundary current emerging from the central plume vortex, taken 10 cm from the end of the channel. $W = 10$ cm, $H = 12.5$ cm, $f = 0.8\ \mathrm{s}^{-1}$, $B_0 = 37.24\ \mathrm{cm}^4/\mathrm{s}^3$, $H/L_f = 4.3$, $Re = 350$. Note the boundary current in the top right, and the plume source in the bottom center of the image.

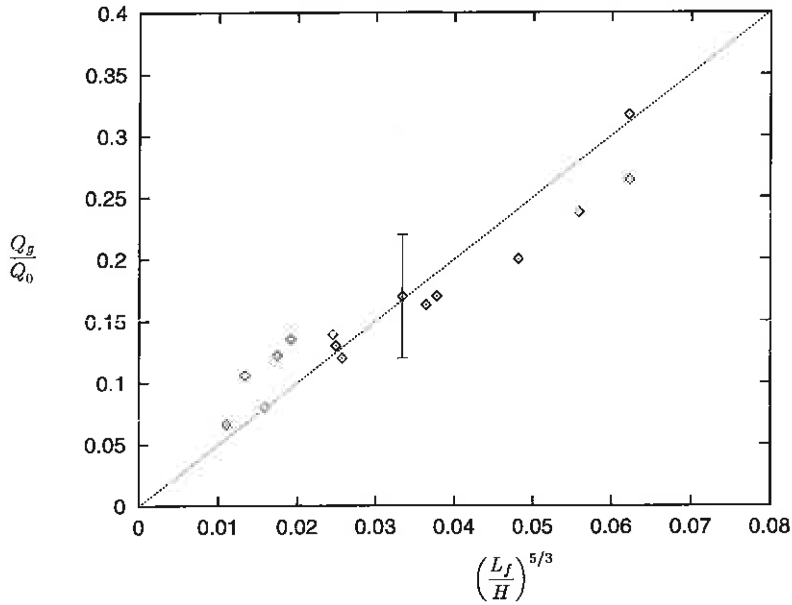

FIGURE 6 The dependence of volume flux, Q_g, exiting the channel in the form of geostrophic gravity currents, on the rotation rate of the system. The dashed line represents $(Q_g/Q_0) = 5.0\ (L_f/H)^{5/3}$. A characteristic error bar is shown.

10 relative to that in the absence of rotation. The experiments indicate that

$$\frac{Q_g}{Q_0} = (5.0 \pm 1.0)\left(\frac{L_f}{H}\right)^{5/3}. \tag{12}$$

This scaling result is consistent with the simple physical model of the plume entraining as it would in the absence of rotation up to a distance $2.6L_f$ above the source, above which rotation serves to suppress entrainment into the plume.

5. STRATIFIED AMBIENT

In a stratified unbounded environment characterized by a constant Brunt-Vaisala frequency N, a turbulent plume rises to a maximum height

$$Z_{\max} = 3.8\,B^{1/4}N^{-3/4} \tag{13}$$

(Turner, 1973). Figure 7 illustrates the dependence of $Z_{\max}$ on the channel width for a plume discharging into a stratified environment bound by an open-ended channel. For sufficiently wide channels, $Z_{\max}/W < 3$, the observed maximum heights are consistent with (13). For more narrow channels, $Z_{\max}$ increases, which suggests that the channel walls are suppressing entrainment into the buoyant plume.

The volume flux at the level of neutral buoyancy may likewise be expressed in terms of B and N through

$$Q_p\,(Z_n) \sim B^{3/4}N^{-5/4}, \tag{14}$$

(Morton *et al.*, 1956). If the plume fluid exits the channel in the form of a pair of high *Re* gravity currents, their exit velocities are given by

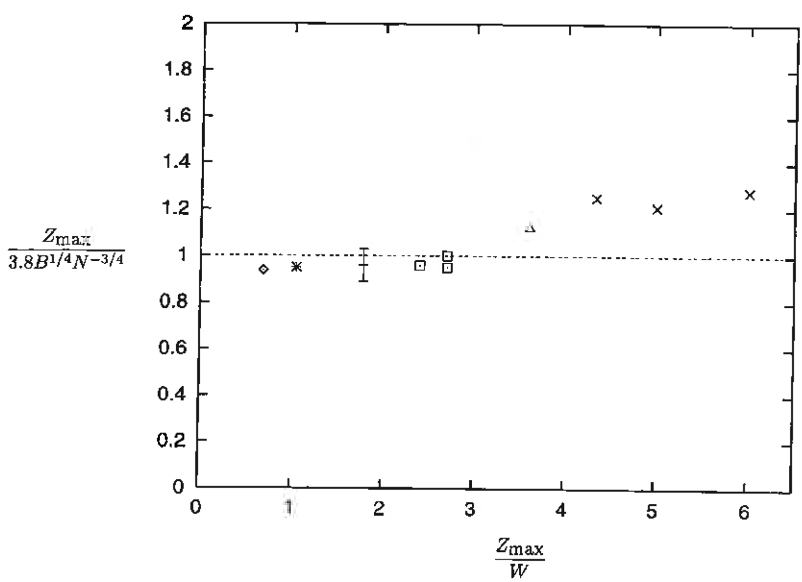

FIGURE 7 Dependence of maximum rise height of a buoyant plume in a stratified ambient on channel width. Symbols $\times$, Δ, $\Box$, $+$, $*$, $\Diamond$ correspond to channels of width 3, 4, 5, 6, 7 and 11 cm, respectively. A characteristic error bar is shown. The horizontal line corresponds to the result expected in an unbounded environment.

$U \sim Nh$. Conservation of volume requires that $Q_p(Z_n) = 2UWh$, from which it can be inferred that

$$h \sim \frac{B^{3/8}}{N^{9/8} W^{1/2}}. \tag{15}$$

In this case, the gravity current thickness depends explicitly on the source conditions.

The gravity current thicknesses were measured in a manner identical to that employed in the homogeneous ambient. In Figure 8, we plot the current depth as a function of $Z_{\max}/W$ for the six channel widths used. The experiments confirm that the scaling (15) is robust over a limited parameter range, and indicate that the constant of proportionality is given by (1.2±0.2). The scaling breaks down in wide channels, where the Reynolds number of the gravity currents $Re < 50$. In this case, there is an additional viscous drag on the current and the gravity

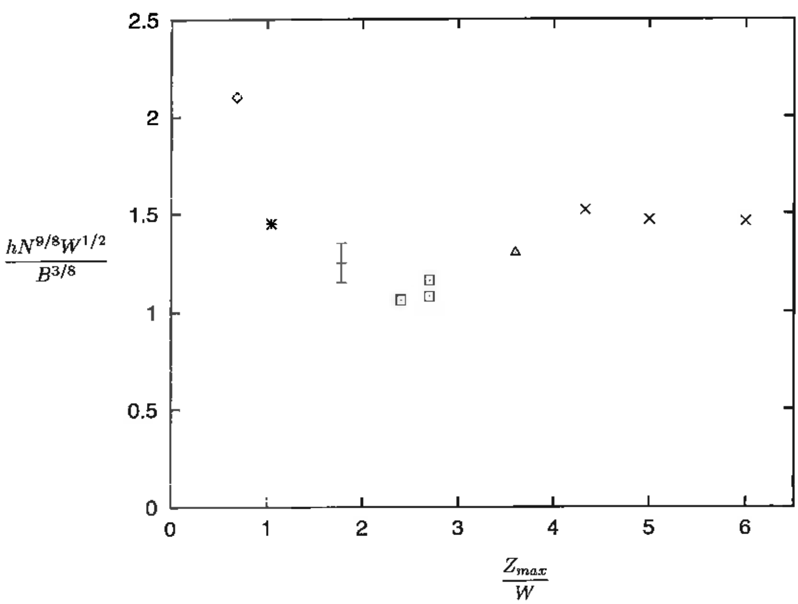

FIGURE 8 The dependence of the thickness of the gravity current, formed by a turbulent buoyant plume discharging into a stratified fluid bound by an open ended nonrotating channel, on the channel geometry. Symbols ×, Δ, □, +, ∗, ◇ correspond to channels of width 3, 4, 5, 6, 7 and 11 cm, respectively. A characteristic error bar is shown.

currents must be thicker in order to transport the same volume of fluid at a slower speed. The scaling (15) likewise breaks down in narrow channels, $Z_{\max}/W > 4$ and does so in a manner consistent with there being diminished entrainment into the plume, as suggested by Figure 7.

When the stratified ambient was rotating, we observed modes of discharge which were analogous to those in the homogeneous environment. At the highest rotation rates, the lenticular neutral cloud above the plume source became unstable before spanning the channel width; consequently, the flow was characterized by the pulsatile shedding of lenticular vortices from the neutral cloud. At lower rotation rates, the neutral cloud spans the entire channel width, and the discharge of plume fluid from the channel is characterized by two counterflowing boundary currents supplied by the neutral cloud. As viewed from above, these modes of discharge thus resemble those arising in the homogeneous ambient and illustrated in Figures 3b and 3c; however, in the stratified environment, all of the discharge from the channel occurs near the level of neutral buoyancy rather than the free surface.

The delineation between the steady and pulsatile regimes was complicated significantly by the influence of viscosity. In the stratified environment, the boundary currents intruding at the level of neutral buoyancy were typically only 1 cm deep and moving at 0.5 – 1.0 cm/s, and so were characterized by moderate Reynolds numbers of $\sim$50, at which viscous effects become important in the dynamics of gravity currents (Simpson, 1997). We were thus unable to model the high *Re* geostrophic flows of interest in the geophysical problem. Dye streaks revealed evidence of counterrotating circular gyres established within the channel, presumably set up by viscous interaction with the central anticyclonic vortex. As the boundary current advances along the channel wall in this moderate *Re* regime, the plume fluid is typically swept off the wall and into the channel interior by one of the gyres. The characterization of the parameter regime in which counterflowing boundary currents arises was thus precluded by the influence of viscosity in our experiments.

While the geostrophic parameter regime could not be reached experimentally in the stratified ambient, it is possible to develop a consistent physical picture for the discharge of a turbulent plume in a rotating, stratified channel by coupling our observations in the homogeneous environment with existing experimental studies of turbulent buoyant plumes in rotating, stratified, and unconfined environments (Helfrich and Battisti, 1991). In particular, we expect that the pulsatile regime will arise in the stratified environment when the channel width exceeds the maximum radius of the neutral cloud defined in (1), $W > R_r$. In this case, the vortices shed by the neutral cloud will propagate away from the source, approach the wall, then propagate towards the end of the channel. When $W < R_r$, the neutral cloud will interact with the channel walls before going unstable. One thus expects a steady flow characterized by a stable anticyclonic neutral cloud sitting above the source, spanning the width of the channel, and leaking fluid in the form of two counterflowing gravity currents which exit the channel.

On the basis of simple geostrophic theory, it is once again possible to make inferences concerning the depth h and thickness d of the steady boundary currents exiting the channel. In this case, the geostrophic balance in the boundary current of height $h(x)$ yields

$$u(x) = \frac{N^2}{f} h \frac{dh}{dx}, \tag{16}$$

so that the volume flux in the currents is given by

$$Q_g = \int_0^w uh\, dx = \frac{N^2}{3f} h_0^3. \tag{17}$$

In the oceanographic setting, $N \gg f$, and the plume rise time is much shorter than a day; consequently, we assume that the entrainment into the plume is influenced by neither rotation nor stratification. If one assumes that $Q_g = Q_p/z$, where Q_p is defined in (13), then the maximum depth of a boundary current in the stratified system would be

$$\frac{h}{H} \sim \left(\frac{f}{N}\right)^{1/3}. \tag{18}$$

Moreover, the thickness d of the geostrophic gravity current exiting the channel is obtained by noting that $d \sim Nh/f$, so that

$$\frac{d}{H} \sim \left(\frac{N}{f}\right)^{2/3} \tag{19}$$

6. DISCUSSION

We have investigated the combined influence of a bounding channel geometry and rotation on the dynamics of buoyant plumes discharging into both homogeneous and stratified ambients. The dependence of the mode of discharge of plume fluid from the channel on the governing parameters has been delineated. The principal results are summarized in Table I. The flows are typically characterized by steady counterflowing gravity currents; however, pulsatile regimes have also been identified at the highest rotation rates. The onset of time-dependence in the flow is brought on by instability of the anticyclonic vortex overlying the source, either the columnar vortex in the homogeneous environment, or the lenticular neutral cloud in the stratified case. The criterion for the transition between steady and pulsatile flows thus depends on the relative magnitudes of the channel width and the maximum radius attainable by the plume structure. If the plume structure can grow to a radius exceeding the channel width, then the plume fluid may exit the channel by way of geostrophic boundary currents, and a steady state may be maintained.

Our investigation of the homogenous environment has also allowed us to make an important inference concerning the influence of rotation on entrainment into a turbulent plume. In the regime characterized by counterflowing surface currents, we were able to compute the volume

TABLE I A characterization of the modes of discharge of buoyant plume fluid released from within an open-ended channel of width W in a system rotating with angular speed $\Omega = f/2$. In the homogeneous ambient, the form of the flow is determined by the magnitude of the lengthscale L_f. In the stratified ambient, the critical lengthscale is the maximum radius attainable by the neutral cloud, R_r, before the onset instability

	Homogeneous Ambient	*Stratified Ambient* ($N \gg f$)
$f=0$	currents of depth $h=(0.13\pm0.02)\ H^{5/3}W^{-2/3}$ counterflowing at surface	currents of thickness $h=(1.2\pm0.2)\ B^{3/8}N^{-9/8}W^{1/2}$ counterflowing at a depth $Z_n=(3.8\pm0.2)\ B^{1/4}N^{-3/4}$
moderate f steady flow	Criterion: $W < (8.0\pm0.5)L_f$ counterflowing surface boundary currents	Criterion: $W < R_r$ counterflowing boundary currents at depth Z_n
high f pulsatile flow	Criterion: $W > (8.0\pm0.5)L_f$ shedding of columnar anticyclonic vortices	Criterion: $W > R_r$ shedding of lenticular anticyclonic vortices

flux exiting the channel from the depth of the currents, and so infer the total amount of fluid being entrained into the plume. Our result (12) is consistent with the plume entraining as in the absence of rotation until it reaches a height $2.6L_f$ above the source, beyond which the dynamics is dominated by rotation: the plume becomes columnar, and the radial entrainment into the plume is completely suppressed. While such an inference has important implications in a variety of geophysical problems, it is important to note that the coefficient 2.6 may not be entirely reliable since the observed decrease in entrainment with increasing rotation rate may also have been influenced by the channel geometry.

Hydrothermal plumes at mid-ocean ridges play an important role in deep-ocean mixing and the chemical and thermal budget of the oceans (Edmond *et al.*, 1979); moreover, they are responsible for the deposition of precious metals and the sustenance of novel ecosystems at the seafloor (Kim *et al.*, 1994). Mineral-laden hydrothermal effluent emerges from sulphide structures on the sea-floor in the form of turbulent buoyant plumes which rise typically 200 – 300 metres through the stratified ocean depths until reaching its level of neutral buoyancy and spreading as a gravity current. Weaker, more diffuse outflows also arise, leading to effluent being confined lower in the water column. Many hydrothermal plume fields arise in axial valleys which are typically several kilometres wide and up to a few hundred metres deep and so place an important constraint on the dynamics of the hydrothermal fluid. We conclude by considering the combined influence of the Earth's rotation and the channel geometry on the dispersal of hydrothermal effluent from axial valleys.

Our model suggests that the nature of the discharge of hydrothermal effluent from axial valleys depends explicitly on the ratio of the channel width W to the maximum radius attainable by the neutral cloud, R_r, defined in (1). For $W/R_r > 1$, the dispersal will be episodic, and characterized by the motion of lenticular eddies with height to radius aspect ratio $h/R \sim f/N$, which will spin down after a time $\tau_s \sim (h/\Omega\nu)^{1/2}$. For $W/R_r < 1$, hydrothermal effluent will exit the axial valley in the form of two counterflowing boundary currents. Typically, axial valleys are several kilometres wide, and black smoker plumes intrude to heights of 200 – 300 metres. If the smoker plumes do not rise above the valley wall, then one expects the neutral cloud to attain a radius of order $R_r \sim NZ_n/f$ which will typically be several kilometres in the deep ocean. The experimental results reported herein imply that the discharge of hydrothermal effluent from axial valleys may therefore be characterized by either counterflowing boundary currents of characteristic width b, or the episodic release of lenticular eddies.

Kim *et al.* (1994) have suggested that smoker plumes play an important role in the migration of various vent species, through the disperal of larvae from one vent site to another. They have argued that the larval pathway consists of entrainment into the smoker plume, transport to the neutral height, then precipitation to another vent site on the seafloor. As the larvae are effectively passive throughout this journey, the survival of the vent species depends crucially on the form of the plume-induced flow. The physical picture presented herein thus has significance in constraining the migration patterns of these species. The scenario characterized by geostrophic boundary currents will give rise to preferential precipitation of larvae near one side of the valley. Moreover, migration along vents aligned with the middle of the valley will not be facilitated if $b \ll W/2$. The physical picture described herein will likewise impact the patterns of mineral deposition by hydrothermal effluent: one expects minerals to precipitate out preferentially on one side of the channel. Moreover, one expects that the along-channel entrainment flow may have an impact on particle recycling from the exiting gravity currents. As a caveat, we note that the physical picture described herein of dispersal of hydrothermal effluent from smoker plumes in an axial valley has been developed on the assumption that there is no ambient flow. Currents in the vicinity of the seafloor have typical speeds of $1-10$ cm/s, and their influence on the dynamics of hydrothermal plumes has recently been considered by Lavelle (1997). We expect that strong ambient currents will change the physical picture described herein, and will lead to significantly more complex dispersal patterns.

Acknowledgements

The authors gratefully acknowledge financial support from NERC BRIDGE grant GST/02/1147.

References

Baines, W. D. and Turner, J. S., "Turbulent buoyant convection from a source in a confined region," *J. Fluid Mech.* **37**, 51–80 (1969).

Edmond, J. M., Measures, C., McDuff, R. E., Chan, L. H., Collier, R., Grant, B., Gordon, L. I. and Corliss, J. B., "Ridge crest hydrothermal activity and the balances of the major and minor elements in the ocean: The Galapagos data," *Earth Planet. Sci. Lett.* **46**, 1–18 (1979).

Fernando, H. J. S., Chen, R.-R. and Boyer, D. L., "Effects of rotation on convective turbulence," *J. Fluid Mech.* **228**, 513–547 (1991).

Griffiths, R. W. and Hopfinger, E. J., "Gravity currents moving along a lateral boundary in a rotating fluid," *J. Fluid. Mech.* **134**, 357–399 (1983).

Griffiths, R. W. and Linden, P. F., "The stability of vortices in a rotating, stratified fluid," *J. Fluid. Mech.* **105**, 283–316 (1981).

Helfrich, K. R. and Battisti, T. M., "Experiments on baroclinic vortex shedding from hydrothermal plumes," *J. Geophys. Res.* **96**, 12511–12518 (1991).

Kim, S. L., Mullineaux, L. S. and Helfrich, K. R., "Larval dispersal via entrainment into hydrothermal vent plumes," *J. Geophys. Res.* **99**(C6), 12655–12665 (1994).

Lavelle, J. W., "Buoyancy-driven plumes in rotating, stratified cross flows: plume dependence on rotation, turbulent mixing and cross-flow strength," *J. Geophys. Res.* **102**, 3405–3420 (1997).

Linden, P. F. and Cooper, P., "Multiple sources of buoyancy in a naturally ventilated enclosure," *J. Fluid Mech.* **311**, 177–192 (1996).

Linden, P. F. and Simpson, J. E., "Continuous releases of dense fluid from an elevated point source in a cross-flow," In: *Mixing and transport in the environment* (Eds. Beven, K. J., Chatwin, P. C. and Millbank, J. H.) J. Wiley and Sons (1994).

Maxworthy, T. and Narimousa, S., "Unsteady, turbulent convection into a homogeneous, rotating fluid, with oceanographic applications," *J. Phys. Oceanogr.* **24**, 865–887 (1994).

Morton, B. R., Taylor, G. I. and Turner, J. S., "Turbulent gravitational convection from maintained and instantaneous sources," *Proc. Roy. Soc. Lond.* **234**, 1–23 (1956).

Simpson, J. E., *Gravity currents in the environment and the laboratory*, 2nd edition, Cambridge University Press (1997).

Speer, K. G. and Marshall, J., "The growth of convective plumes at seafloor hot springs," *J. Marine Res.* **53**, 1025–1057 (1995).

Stern, M. E., Whitehead, J. A. and Hua, B. L., "The intrusion of a density current along the coast of a rotating fluid," *J. Fluid. Mech.* **123**, 237–265 (1982).

Turner, J. S., *Buoyancy effects in fluids*, Cambridge University Press (1973).